

Microscopic study of the giant multipole resonances in light deformed nuclei via radiative capture reactions. II

K. W. Schmid

Institut für Kernphysik der Kernforschungsanlage Jülich, D-5170 Jülich, West Germany

G. Do Dang

Laboratoire de Physique Théorique et Hautes Energies, Université de Paris-Sud, F-91405 Orsay, France*

(Received 7 April 1978)

Within the framework of a microscopic theory for the multipole resonances in light deformed nuclei, the radiative capture reaction $^{19}\text{F}(p,\gamma)^{20}\text{Ne}$ is being studied. Accent is being put on improving the formalism of the theory as well as on gauging the relative importance of the quadrupole transitions as compared to the dominant dipole ones. From the results obtained for the cross sections and angular distributions it is seen that the reaction runs predominantly through the giant dipole states. The isoscalar quadrupole resonance is only weakly excited even though intermediate states with large $B(E2)$ values are available. The result may help to understand why in proton radiative capture reactions one detects a different $E2$ -strength distributions as compared to what is observed in α -induced experiments.

<p>NUCLEAR STRUCTURE ^{19}F, ^{19}Ne, ^{20}Ne; calculated spectra, $E1$ and $E2$ transitions. Angular momentum projected deformed ph model.</p> <p>NUCLEAR REACTIONS $^{19}\text{F}(p,\gamma)$; calculated cross sections to ground and first excited states. Giant dipole and quadrupole resonances in ^{20}Ne.</p>

I. INTRODUCTION

In a recent paper¹ (hereafter referred to as I), we proposed a microscopic model for the description of the giant multipole resonances (GMR) in light deformed nuclei and their excitation via radiative proton capture reactions. The model is composed essentially out of two main parts. For the description of the reaction itself, Feshbach's projection operator formalism,² or rather a version of it,³ designed specifically for photo-nuclear reactions, has been used in an essential manner. As is well known, this formalism has the attractive feature that it allows the separation of the nuclear structure part for which we have adopted the projected Tamm-Dancoff model (PTD) proposed earlier⁴ in which the initial, final, and intermediate states are obtained by projecting to good parity, isospin, and angular momentum configurations with one hole and one particle-one hole with respect to a Hartree-Fock deformed basis.

In I, in order to test the model and the feasibility of doing a realistic calculation, the $^{19}\text{F}(p,\gamma)^{20}\text{Ne}$ radiative capture reaction has been studied in some detail. Actually, we have limited ourselves to the electric dipole part (GDR) of the giant resonances, namely, to those intermediate states which can decay by electric dipole transitions to the ground and first excited states of ^{20}Ne and which are believed to be the most important. As a matter of fact, it has been shown that the ex-

citation spectrum, as seen from the 90° yields of both the (p,γ_0) and (p,γ_1) processes, can be reasonably well described by the model, a fact which should give some confidence in the description of both the nuclear structure part as well as the excitation mechanism. The calculation has been at the same time an occasion for testing a number of approximations which are frequently made in the literature. For example, the "final state interaction" has been explicitly calculated and was found, fortunately indeed, to be small as commonly assumed. On the other hand, the nonoverlapping-resonance approximation was shown not to be always valid as in the case of the (p,γ_1) process for which the intermediate states are rather densely populated. Finally, it should be mentioned that, despite the complication due to the angular projection, the numerical work can be done without too much labor.

Encouraged by the results of I, we decided to push further the calculations to look at other aspects of the problem and at the same time to correct some of its deficiencies. As a matter of fact, in our first step, we made a number of approximations and assumptions which, even though physically plausible, are not justified *a priori*. For example, the nuclear structure part could obviously be improved with the present knowledge about the techniques of bound state calculations. Furthermore, as we have already noticed, even though the giant dipole resonances are the main components of the excitation function,

other multipolarities, in particular the quadrupole one, should play a role in the angular distributions. Obviously, a dipole transition alone cannot account for any deviation of the a_1 coefficient from zero. We would mostly like to see whether the inclusion of the quadrupole transitions could improve the agreement of the a_i coefficients with experiment.

In Sec. II, a sketch of the formalism given in I will allow us to point out those places where improvements and/or corrections are being made. The results, at least those which we believe are most representative of the effects brought about by these modifications, are given in Sec. III and their significance with respect to the model is discussed. A fact which most clearly comes out from these results is that the isoscalar quadrupole resonances are only weakly excited. This may help to understand why one detects sometimes so little $E2$ strength in this kind of reaction as compared to what is observed in α -scattering experiments.

II. REACTION MECHANISM AND BOUND STATE CALCULATIONS

We refer to Refs. 1 and 4 for details of the reaction mechanism and the definition of the various bound state configurations. Below, we shall confine ourselves to giving a sketch of the whole calculation in order to point out those modifications, corrections, and additions which are necessary for an improvement of the model.

Following Ref. 3, let us recall that the total Hilbert space is divided into three subspaces p , d , and x . The continuum space p is composed out of all those configurations with one particle in the continuum coupled to a set of low-lying bound states of the $A-1$ system. These states will be defined explicitly in the problem. The capture reaction is then supposed to go through a set of intermediate states, called doorway states, which, together with the final states of the A nucleus, form the d space. All other states with more complicated configurations will be grouped into the x space and are supposed to have only marginal influence on the process under consideration.

Starting from an initial state $|c^*\rangle$ representing a proton incident on an $A-1$ nucleus in its ground state, the capture process leading to a state $|I\rangle$ of the A system has been shown to be defined by the T matrix as

$$T_{I,c}^\gamma = \langle I | H_\gamma | c^* \rangle + \sum_{dd'} [\langle I | H_\gamma | d \rangle + F_{I,d}^\gamma] \times M_{dd'}^{-1} \langle d' | H_{dp} | c^* \rangle. \quad (1)$$

Here, H_γ is the electromagnetic interaction and H_{dp} is formally the total Hamiltonian relating the two spaces d and p . $F_{I,d}^\gamma$, the so called final state interaction term, is given by

$$F_{I,d}^\gamma = \langle I | H_\gamma G_p^{(-)} H_{pd} | d \rangle, \quad (2)$$

with $G_p^{(-)}$ being the Green's function in the p space. Finally, the shift and width matrix M is defined by

$$M_{dd'} = \delta(d, d') [E - E_d - \Delta_x + i\Gamma_x/2] - \langle d | H_{dp} G_p^{(-)} H_{dp} | d' \rangle, \quad (3)$$

where E_d is the energy of the intermediate state d and in which the effect of the x space is approximated by a constant (energy independent) shift Δ_x and width $\Gamma_x/2$.

The calculations of I start essentially from the above formulas by making a number of additional approximations, some of which, as already said above, are not quite satisfactory. We shall now examine in some detail how these deficiencies can be removed.

(i) *On the definition of the continuum space.*

As usual, the motion of the particle in the continuum is supposed to be defined by a local one-body Hamiltonian with the potential taken to be of the Wood-Saxon form. The p space is then obtained by coupling this particle to the hole states of the $A-1$ system. Here, an important approximation is made, namely that the particle-hole states thus defined are diagonal with respect to the total Hamiltonian. In other words, one neglects channel-channel coupling. Such an approximation is known to be valid only when there are no single-particle resonances. When this is the case and if all single-particle wave functions being used in the problem are solutions of the same Wood-Saxon potential, then in the calculation of matrix elements of the form $\langle c | H_{dp} | d \rangle$, only the two-body part of the total Hamiltonian H_{pd} will contribute. However, when single-particle resonances exist as they do in the problem at hand, one way to circumvent the difficulty⁵ is to extract from the resonances quasibound states which are then included in the definition of the d space. Such quasibound states are not eigenstates of the single-particle Hamiltonian and thus can also decay into the continuum through the one-body term. This fact has been emphasized lately by Micklinghoff.⁶ It had been omitted in the calculations of I. In the present calculations, this contribution will be included and its importance will be discussed in the next section.

(i) *On the definition of the bound states.* Let us recall how these states are defined. Starting from the Hartree-Fock state $| \rangle$ in which the lowest

deformed orbitals are occupied, one creates a set of particle-hole states by

$$|M\alpha^{-1}\rangle = a_M^\dagger a_\alpha | \rangle. \quad (4)$$

By coupling to good isospin and parity and using the projection operator⁷ P^{JM} , one obtains the following sets of states:

From $| \rangle$:

$$|J^\pi M_J T=0\rangle = P^{JM} | \rangle \quad (5)$$

From $|M\alpha^{-1}\rangle$:

$$\begin{aligned} & |(M\alpha^{-1})J^\pi M_J T\rangle \\ &= P^{JM} \frac{1}{\sqrt{2}} [(a_M^\dagger a_\alpha | \rangle)_T + (-1)^{J-(m_M-m_\alpha)} (a_M^\dagger a_\alpha^- | \rangle)_T] \quad (6) \end{aligned}$$

which span the whole d space. In I, the set (5), which is nothing but the Hartree-Fock ground state rotational band, has been used for the final states. It is true that for ^{20}Ne , the low-lying spectrum is pretty well described by this simple procedure. There is, however, some inconsistency in the sense that any state of this band is because of the projection, not orthogonal to those of the set (6) with the same quantum numbers $J^\pi T=0$. The mixing of the states between the two sets coming from the diagonalization of the total Hamiltonian may not have drastic influence on their energies but may give rise to finite effects on their electromagnetic properties⁸ and therefore on the radiative capture cross sections. This mixing will be taken into account in the present work, and as a consequence, any state of the d space can now be written in the form

$$\begin{aligned} |d\rangle &= \delta(T, 0) \delta(\pi, +) \delta((-1)^J, 1) C_{0,d}^{J^\pi T} |J^\pi M_J T=0\rangle \\ &+ \sum_{\substack{\alpha \leq F \\ M > F}} C_{\alpha M, d}^{J^\pi T} |(M\alpha^{-1})J^\pi M_J T\rangle. \quad (7) \end{aligned}$$

Now, concerning the states (6) obtained from the particle-hole configurations, another restriction has been made in I, namely, that there was no mixing between configurations with the projection $K = m_M - m_\alpha$ differing by an odd number, namely, that the rule $\Delta K = \text{even}$ was required. It is true that this rule is exactly satisfied in the intrinsic basis. However, as the diagonalization of the total Hamiltonian is carried out after projection and as the rotation operator connects states with even and odd K , the restriction $\Delta K = \text{even}$ is no longer valid.⁹ It will, therefore, be removed in the present work.

(i) *On the electromagnetic interaction.* It is a well known fact that if the $E1$ transition is not strictly forbidden by some selection rule in any electromagnetic process, it will be the dominant one. This obviously was the underlying idea in

I for neglecting all other multiplicities in the γ -decay process, except the electric dipole one. There was, however, from the numerical point of view, another less important reason behind this simplification: As the dipole operator carries $\Delta J=0, 1$, $\Delta T=1$, and $\pi=-$, and as all the final states are $T=0$ positive parity states, all intermediate states (of the d space) must have $T=1$ and negative parity. Thus, from the set (6), all other states with $T=0$ and/or $\pi=+$ could be neglected.

In the energy region of the giant resonance, the above simplifying assumption is probably justified, as it is capable of reproducing the main features of the excitation spectrum. Other experimental data, however, depend more sensitively on the admixture of other multiplicities, as for example, the angular distribution. Writing the differential cross section in the form

$$\frac{d\sigma(N, \gamma)}{d\Omega} = a_0 \left(1 + \sum_{Q \geq 1} a_Q P_Q(\cos \theta) \right), \quad (8)$$

the experimentally measured values of a_Q will tell us how much mixing is involved. A nonzero value of a_1 , for example, cannot be explained by the $E1$ transition alone. In I, we have already noticed that the agreement between theory and experiment was rather poor. The question is, then, whether one could improve the agreement by including, say, the quadrupole transition, which is the next most important. This is what we shall do in this work, as we believe that, no matter what the answer will be, it will tell us the way to proceed further.

It should be remarked that the effect of all the above modifications is to lengthen somewhat the numerical part of the calculations but does not raise any formal difficulty. The ingredients for computing the various matrix elements involved are already given in detail in I, and by relaxing some of the restrictions on the choice of the d -space configurations, their number and dimension increase somewhat but still remain within acceptable limits.

III. RESULTS FOR THE $^{19}\text{F}(p, \gamma)^{20}\text{Ne}$ REACTION AND DISCUSSIONS

In order to have an idea of the effect brought about by the modifications explained in the previous section and to compare the results with experiment, we shall take up again the study of the radiative capture reaction $^{19}\text{F}(p, \gamma)^{20}\text{Ne}$. Most of the parameters being used in this work to define the bound and continuum spaces as well as their coupling are the same as those of I. Based on our experience with the previous work, some of them have, how-

ever, been slightly modified, partly in an effort to get better agreement with experiment and also to make the calculations more consistent with our present formulation of the problem.

Let us first consider the nuclear structure part. The configuration space is defined by the $0p$ -, $1s0d$ -, and $0f$ -spherical orbits, with the $1p$ orbit being excluded, as no p -wave resonances exist which would permit the extraction of quasibound states.⁵ The parameters for the effective Hamiltonian inside the $1s0d$ shell have been taken from the work of Halbert *et al.*¹⁰ They use the values $\epsilon_{d_{5/2}} = -4.49$, $\epsilon_{s_{1/2}} = -3.16$, and $\epsilon_{d_{3/2}} = 1.05$ for the single-particle energies relative to the ^{16}O core, and a modified surface δ interaction (MSDI) with $A_{T=0} = 0.77$, $A_{T=1} = 0.95$, $B_{T=0} = -2.51$, and $B_{T=1} = 0.37$. All energies are in MeV. It is important to remark that the MSDI, with the above parameters, has been designed uniquely for the sd shell. In I, exactly the same interaction has been used for the whole space under consideration. As a result, in order to reproduce the $\frac{1}{2}^+ - \frac{1}{2}^-$ spacing in the $A=19$ system, the single-particle energies of the $0p$ shell have been chosen to be about 3 MeV higher than the experimental values, namely $\epsilon_{p_{3/2}} = -21.74$ and $\epsilon_{p_{1/2}} = -15.60$. This procedure corrects only the diagonal part of the two-body interaction. By comparing it with other phenomenological interactions, the MSDI is seen to be too strong for the $0p$ shell, and even more so when used as a coupling potential between the $0p$ and $1s0d$ shells. As a result, we have decided to adopt the experimental single-particle energies for the $0p$ and modified instead the monopole terms B_T to be $B_{T=0}(p, sd) = -1.475$ and $B_{T=1}(p, sd) = 1.075$. Of course, the same kind of adjustment could be done for the sd - f interaction. However, as there is no experimental information for this purpose, the original MSDI will be retained as such, and any adjustment will be supposed to be absorbed in the $0f$ single-particle energies. In I, two sets of values have been chosen, and the results hint to something slightly larger than the second lower one. We therefore choose for this work $\epsilon_{f_{7/2}} = 8.5$ and $\epsilon_{f_{5/2}} = 12.5$.

With the above choice of parameters, the Hartree-Fock problem is then carried out in a straightforward manner. Of course, the positive parity orbits come out exactly as in I. For the $0p$ orbits, with the choice given above for B_T and for the single-particle energies, the results are also nearly the same. Note that we always neglect mixing between $0p$ and $0f$ orbits. On the other hand, as a result of the larger values for the $0f$ energies, the corresponding orbits come out somewhat higher, by about 1 MeV. The same features are found for the spectrum of the $A=1$ target sys-

tem. As we are only interested in the few (six) low-lying states, the results are still practically the same as in I, and are in fair agreement with experiment. As we think that the trends brought about by the above slight modification of the parameters could be more or less expected *a priori*, it would be unnecessary to present the corresponding figures.

Now, with the single-particle orbits, we construct the Hartree-Fock determinant $|\rangle$ and the $1p$ - $1h$ states $|M\alpha^{-1}\rangle$. These are then projected to good parity π , isospin T , and angular momentum J , according to the prescription given in I. States with the same $J^{\pi}T$ are then diagonalized in the total Hamiltonian with the characteristics given above. As far as the odd-parity states are concerned, one observes a slight separation of the part of the spectrum coming from the $0f$ particle- sd hole configurations as a result of the increase of the $0f$ single-particle energies. The smaller changes observed in the lower part of the spectrum are due both to the different choice of the $0p$ - $1s0d$ Hamiltonian and to the relaxation of the ΔK condition. The wave functions of the individual states, however, remain practically the same, and as we shall see below, the resulting dipole part of the $^{19}\text{F}(p, \gamma)^{20}\text{Ne}$ cross section looks very much like the one obtained in I. Actually, we are more interested in the results for the even-parity states, namely, the $J^{\pi} = 0^+, 1^+, 2^+, 3^+, 4^+$, $T=0, 1$ which can decay to the ground and first 2^+ states by quadrupole transitions. A point should be mentioned here concerning the effective interaction being used for the diagonalization. As said above, the MSDI with the given parameters has been chosen to fit the experimental results for the sd shell. As such, it is supposed to have already included the effect of the core polarization, namely, of excitations of the form $(0f)(0p)^{-1}$. In our problem, however, these configurations are being explicitly introduced for the construction of positive parity states. As a result, in order to avoid a kind of double counting, we decide to neglect all the matrix elements connecting the $(sd)(sd)^{-1}$ and $(0f)(0p)^{-1}$ configurations.

Figure 1 gives the result for the ground state band of ^{20}Ne . The effect of the mixing with the projected particle-hole states is an energy gain of 350 keV from the simple Hartree-Fock rotational band, and brings the result to better agreement with experiment. A slight improvement is also obtained for the "dynamic" quadrupole moments defined as

$$Q_{I'I}^{\text{dyn}} = \left(\frac{16\pi}{5} B(E2, I \rightarrow I') \right)^{1/2} (\langle II'00 | 20 \rangle)^{-1}. \quad (8)$$

Note that, for the calculation of these dynamic

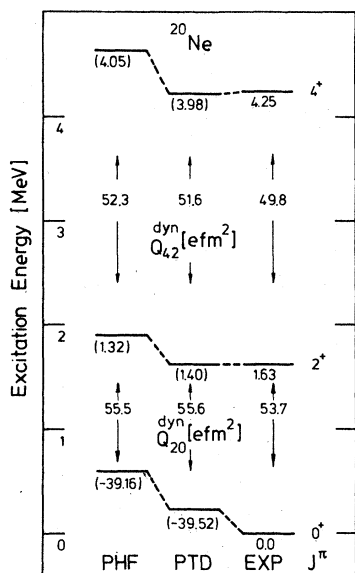


FIG. 1. The ground state band of ^{20}Ne . The theoretical energy values obtained by projecting angular momentum from only the Hartree-Fock vacuum (PHF) are compared with those from the multideterminantal angular momentum projected particle-hole model (PDT) and with the experimental data (Ref. 14). Furthermore, the dynamical quadrupole moments as obtained from the measured and calculated $B(E2)$ values via Eq. (4) are presented.

quadrupole moments, an effective extra charge β has been introduced with $\beta=0.5$. The $B(E2)$ values with $\beta=0$ for transitions from the 2^+ , $T=0,1$ to the ground state are given in Fig. 2. The $T=1$ states appear to be about 10 MeV higher than the $T=0$ states. It is interesting to remark that there are a number of isoscalar quadrupole states with strong $B(E2)$ transitions to the ground state. In-

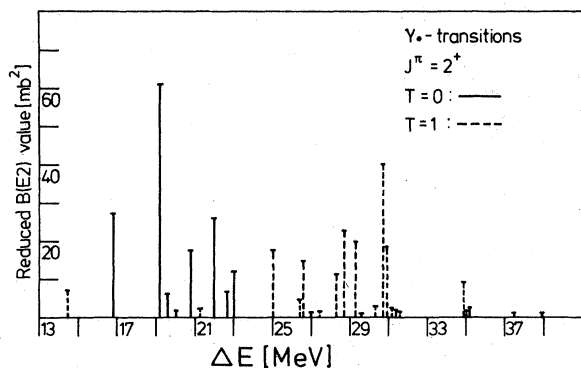


FIG. 2. The reduced $B(E2)$ values for the γ_0 transitions of various $J=2^+$ excited states to the ground state of ^{20}Ne are given. Full lines refer to isoscalar, dashed ones to isovector transitions. The $B(E2)$ values include a phase space factor, so that, if multiplied by $(2J+1)\Delta E$ their contribution to the total photoabsorption cross section can be obtained.

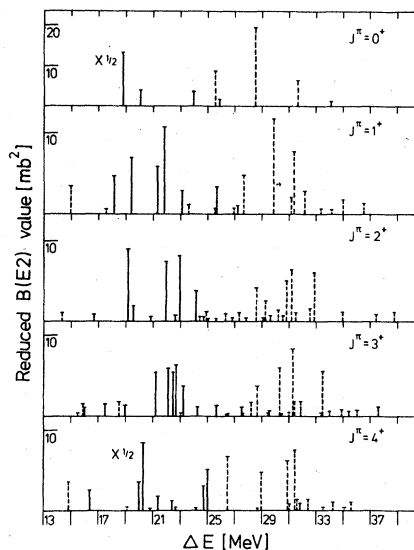


FIG. 3. Same as in Fig. 2, but now for the γ_1 transitions leading to the first excited 2^+ state in ^{20}Ne . The excitation energies of the various $J^\pi=0^+, 1^+, 2^+, 3^+, 4^+$ states are given with respect to the ^{20}Ne ground state.

creasing the value of the effective charge, say, to $\beta=0.5$ again multiplies these transition probabilities by a factor of 4, but leaves the isovector transitions unchanged.

Figure 3 shows the quadrupole transitions to the first 2^+ from states with $J^\pi=0^+, 1^+, 2^+, 3^+, 4^+$ and $T=0,1$. As for the ground state transitions, we observe similar features with isoscalar and isovector strengths concentrated into groups separated by about 10 MeV. Note that considerable isoscalar strengths are found in the same energy region of the dipole transitions.

With the above, the nuclear structure part of the problem is completely defined. To get the T matrix and the cross section, we shall need the continuum wave functions and the coupling Hamiltonian H_{pd} between the bound and continuum spaces. For this part of the problem, we shall adopt exactly the same parameters as in I, namely, on the one hand a Wood-Saxon potential with parameters given by Afnan¹¹ for the scattering waves and, on the other hand, a δ interaction given by Wang and Shakin³ as coupling Hamiltonian. As explained in Sec. II, aside from the two-body interaction, the Wood-Saxon one-body term also gives a contribution to the matrix elements between the two spaces. Actually, as the bound state wave functions of the chosen Wood-Saxon potential are practically identical to the corresponding oscillator ones of the d space, non-negligible one-body matrix elements are to be expected only from the $d_{3/2}$ -proton and $f_{7/2}$ - and $f_{5/2}$ -proton and neutron orbits. Finally, the cou-

pling of the doorway space to the complicated x space is approximated by the energy-independent parameters $\Delta_x = 0$ and $\Gamma_x = 100$ keV.

In I, a number of approximations have been tested. It has been found that the final state interaction term Eq. (2) was negligible. The same is still true in the present calculation, even after taking into account the one-body contribution to the transition matrix elements. It is important to remark, however, that this term, as well as the direct term in Eq. (1), depends strongly on the actual choice of the continuum and doorway spaces. For the dipole Hamiltonian, for example, as the doorway space is rather complete, the direct term has been found to be negligible. The same is no longer true for quadrupole transitions, of course, because starting from the sd shell, the quadrupole operator can lead to quite a number of states which are outside of the space being chosen for the calculation. We have also tested the validity of the isolated resonance approximation in which the M matrix, Eq. (3), is supposed to be diagonal, as compared to the complete calculation where it is effectively inverted. In the following, most of the results are given for the latter procedure, except where we feel that there would be no difference between the two calculations.

Figure 4 shows the 90° -yield curves for the $^{19}\text{F}(p, \gamma_0)^{20}\text{Ne}(0^+)$ reaction for proton energies between 2 and 13 MeV. The experimental results are from the Argonne group.¹² The theoretical calculation reproduces the qualitative feature of the cross section, including the most pronounced peak at 5.15 MeV, but fails to give the right spacing between the three peaks below and the numerous structure observed above. Compared to our previous results, there is now less strength concentrated in the region above 5.5 MeV. This is due to the different choice of the $0f$ single-particle energies, as well as to the one-body term. The quadrupole part contributes practically nothing in this energy region (on the scale of the figure, its effect is unobservable). That the $E2$ part of the electromagnetic interaction contributes at all, however, can be seen from the nonvanishing a_1, a_3, a_4 coefficients in the expansion (8), which are given, together with the a_2 coefficient, in Fig. 5. Aside from the a_2 coefficient, which depends mostly on the dipole transition and for which the agreement with experiment is roughly of the same quality as for the cross section, the other coefficients are rather poorly reproduced. This probably points to some deficiency in the description of the positive parity intermediate states. Above 12 MeV, when the dipole contribution starts to die off, the quadrupole one continues to increase

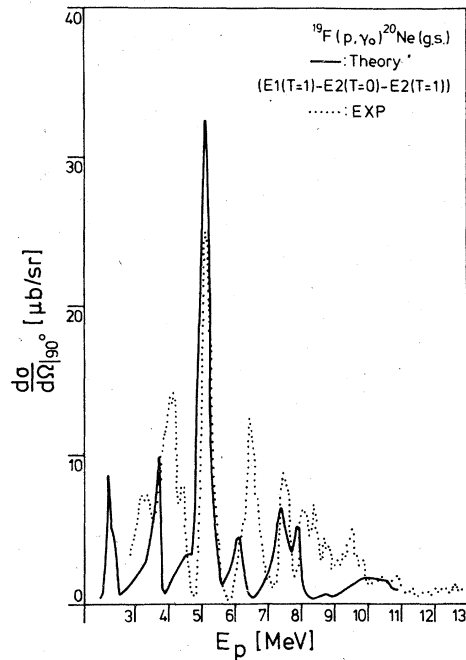


FIG. 4. Experimental (Ref. 12) and theoretical 90° -yield curves for the $^{19}\text{F}(p, \gamma_0)^{20}\text{Ne}$ reaction.

and reaches a maximum at about 27 MeV. Figure 6 presents the result for the pure $E2$ total cross section in the isolated resonance approximation for the whole energy region from 3 to 27 MeV. It shows some structures at about 20 MeV coming from the isovector transitions. Note that the result has been obtained with $\beta = 0$. However, the lower part of the curve is so small that, increasing β to 0.5, which would multiply this part by a factor of 4, one would still find it negligible compared to the dipole contribution. The higher isovector part of the curve remains unchanged. This is to be compared with (α, α') scattering experiments where much more $E2$ strength is observed.¹³ Actually, in the (α, α') process, isoscalar states, in particular the $J^\pi = 2^+$ states with strong $B(E2)$ values to the ground state, are easily excited no matter what their individual structure may be. However, the (p, γ) reactions are much more selective. In the special case of ^{19}F , because of the target spin $\frac{1}{2}^+$, only d waves of the incoming particle can couple with it to reach the 2^+ state. Such configurations are only weakly coupled to the $(0p)^{-1}(pf)$, at least with our δ interaction. As in the energy region of interest, most of the states are mainly of the $(pf)(0p)^{-1}$ nature, so one can now understand why so little $E2$ strength is observed in the process.

Figure 7 now gives the 90° yield curves for the (p, γ_1) reaction leading to the first 2^+ state. Though a number of peaks with reasonable mag-

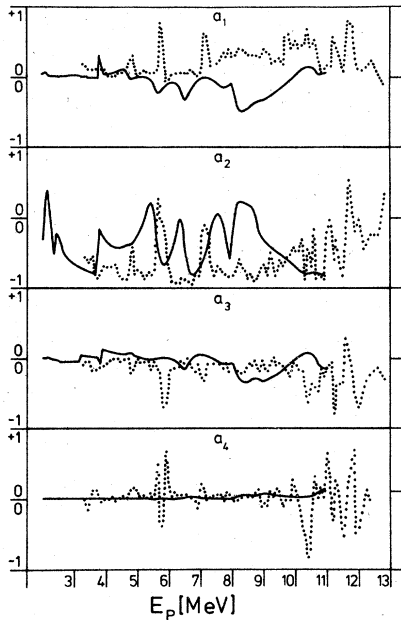


FIG. 5. Measured (Ref. 12) and calculated angular distributions in the $^{19}\text{F}(p, \gamma)^{20}\text{Ne}$ channel

nitude are found, the agreement with experiment is at best qualitative. Given the microscopic nature of the calculation and the few parameters at our disposal (remember the choice of the energy independent values Δ_x and Γ_x) one could hardly expect to reproduce the complicated structures of the experimental curve. The quadrupole part contributes practically nothing, a result which is in agreement with the vanishing of the experimental a_1, a_3, a_4 coefficients.

Finally, in Table I, we give the integrated (γ, p_0) cross sections together with the experimental values.¹² While for the γ_0 channel the agreement is reasonable, the theoretical value for the γ_1 channel is off by a factor of 2. Note that we have not really tried to fit some of these values,

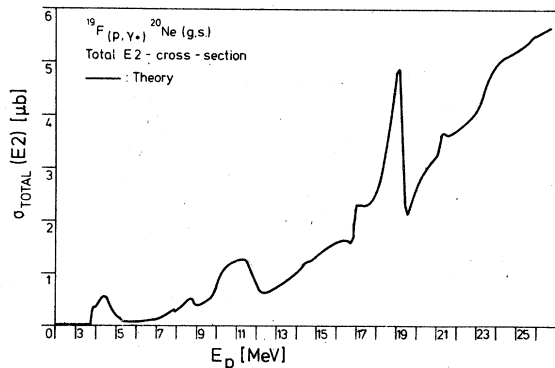


FIG. 6. The calculated $E2$ part of the total $^{19}\text{F}(p, \gamma)^{20}\text{Ne}$ cross section.

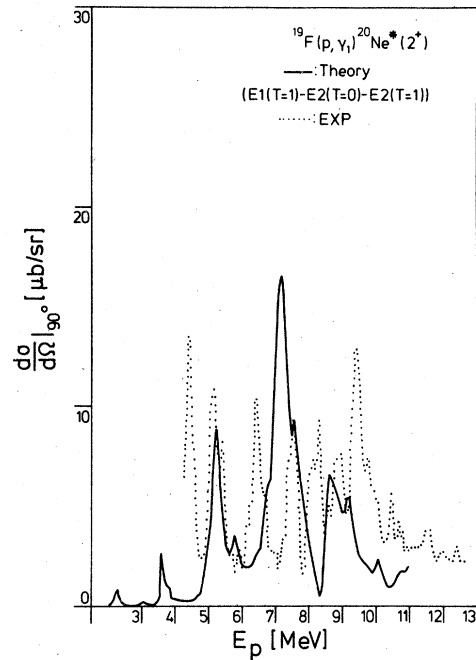


FIG. 7. Experimental (Ref. 12) and theoretical 90° -yield curves for the γ_1 channel of the proton radiative capture reaction on ^{19}F .

say, by changing Γ_x or by any other method.

IV. CONCLUSION

In a previous paper,¹ a model for the description of the giant multipole resonances in light deformed nuclei was proposed. In its application to the study of the radiative capture reaction $^{19}\text{F}(p, \gamma)^{20}\text{Ne}$,

TABLE I. Experimental (Ref. 12) and theoretical values for the integrated total (γ, p_0) cross sections. For the theoretical sums, incident proton energies between 2 and 11 MeV have been considered. The experimental proton energies start at 2.88 MeV for the γ_0 and 4.1 MeV for the γ_1 channel and go up to 12.88 MeV.

Method	J_1^π	J_f^π	$E\lambda$ poles	$\int \sigma_{\gamma, p_0}(E) dE$ (MeV mb)
Theory	0^+	1^-	$E1$	18.5
	(γ_0)	$1^-, 2^+$	$E1 + E2$	18.7
		2^+	$E1$	4.7
	(γ_1)	$1^-, 2^-, 3^-, 0^+, 1^+, 2^+, 3^+$	$E1 + E2$	4.7
		4^+	$E1$	0.5
	(γ_2)	$3^-, 2^+, 3^+$	$E1 + E2$	0.5
Experiment	0^+	All	All	24.8
	(γ_0)			
	2^+	All	All	9.6
	(γ_1)			

the model has been rather successful in reproducing the main features of the dipole strength functions but has failed in the description of the individual states and of the angular distributions. A number of approximations and simplifications have been made in this work which, even though physically, are by no means satisfactory *a priori*. Before going further in the direction of improving the nuclear structure and/or the reaction part of the formalism itself, it would be desirable to assess whether these deficiencies play any role at all in the partial failure of the theory. This is precisely the purpose of the present work. The ground state correlations have therefore been taken into account by allowing the mixing of states obtained from the projection of the Hartree-Fock vacuum and of particle-hole configurations. For the latter, the restriction on the K quantum number has been removed. For the reaction part, an omission in the previous work in neglecting the one-body decay term coming from the nonorthogonality between bound and continuum states has been corrected. Finally, in addition to the dipole part of the electromagnetic interaction, the quadrupole operator has also been included.

From the results obtained in the previous section, it can be seen that all the above corrections are not crucial in the improvement of the theory. They do indeed lead to quantitative changes of the results, but are far from being able to reproduce

the detailed features of the experimental data. Qualitatively, the quality of the agreement between theory and experiment is still practically the same.

It is our belief that any further effort in improving the theory should be directed toward a better description of the nuclear structure part of the calculations. Some of the parameters of the problem should be more carefully chosen, in particular the single-particle energies and effective interactions. Furthermore, though the 1p-1h description of the negative parity states is reasonable, the positive parity states probably involve much more complicated structures, as for example 2p-2h configurations inside of the sd shell.

On the other hand, as a by-product, our calculation has led to a partial understanding of the puzzle about the $E2$ strengths, namely, why one sees so little of these in radiative capture reactions as compared to (α, α') experiments. Though there exist quite a number of states with large $B(E2)$ values to either the ground or the first excited states, they are only weakly excited in the capture process. For a complete answer to the problem, one must however await a calculation for the (α, α') reaction itself, using for example a DWBA analysis with spectroscopic factors obtained from our model.

One of the authors (K.W.S.) would like to thank Professor Faessler, Professor Speth and Dr. Knöpfle for helpful discussions.

*Laboratoire associé au Centre National de la Recherche Scientifique.

¹K. W. Schmid and G. Do Dang, Phys. Rev. C 15, 1515 (1977).

²H. Feshbach, Ann. Phys. (N.Y.) 5, 357 (1958); 19, 257 (1962).

³W. L. Wang and C. M. Shakin, Phys. Rev. C 5, 1898 (1972).

⁴K. W. Schmid and G. Do Dang, Z. Phys. A276, 233 (1976).

⁵W. L. Wang and C. M. Shakin, Phys. Lett. 32B, 421 (1970).

⁶M. Micklinghoff, Nucl. Phys. (to be published).

⁷F. Villars, in *Proceedings of the International School of Physics, Enrico Fermi Course 36*, edited by C. Bloch (Academic, New York, 1966).

⁸K. W. Schmid, S. Krewald, A. Faessler, and L. Satpathy, Z. Phys. 271, 149 (1974).

⁹K. W. Schmid and H. Mütter, Phys. Rev. C 16, 2050 (1977).

¹⁰E. Halbert, J. B. McGrory, B. H. Wildenthal, and S. P. Pandhya, Adv. Nucl. Phys. 4, 316 (1971).

¹¹I. R. Afnan, Phys. Rev. 163, 1016 (1967).

¹²R. E. Segel, Z. Vager, L. Meyer-Schützmeister, P. P. Singh, and R. G. Allas, Nucl. Phys. A93, 31 (1967).

¹³S. S. Hanna, in *Proceedings of the International Conference on Nuclear Structure and Spectroscopy, Amsterdam, 1974*, edited by H. P. Blok and A. E. L. Dieperink (Scholar's Press, Amsterdam, 1974).

¹⁴F. Ajzenberg-Selove, Nucl. Phys. A190, 1 (1972).